A comparison of pre-Millennium eruption (946 AD) and modern temperatures from tree rings in the Changbai Mountain, northeast Asia

Running Title: Millennial changes in temperature of Changbai Mt.

Haibo Du[1], Michael C. Stambaugh[2], Jesús Julio Camarero[3], Mai-He Li[1,4], Dapao Yu[5], Shengwei Zong[1], Hong S. He[2*], Zhengfang Wu[1*]

[1] Key Laboratory of Geographical Processes and Ecological Security in Changbai Mountains, Ministry of Education, School of Geographical Sciences, Northeast Normal University, Changchun 130024, China

[2] School of Natural Resources, University of Missouri, Columbia, Missouri, USA

[3] Instituto Pirenaico de Ecología, IPE-CSIC, 50059 Zaragoza, Spain

[4] Swiss Federal Institute for Forest, Snow and Landscape Research WSL, 8903 Birmensdorf, Switzerland

[5] CAS Key Laboratory of Forest Ecology and Management, Institute of Applied Ecology, Chinese Academy of Sciences, Shenyang, 110016, China

***Correspondence to*:** wuzf@nenu.edu.cn; HeH@missouri.edu

Abstract: High-resolution temperature reconstructions in the prior millennium are limited in northeast Asia, but important for assessing regional climate dynamics. Here, we present, for the first time, a 202-year reliable reconstruction of April temperature before the Millennium volcanic eruption in 946 AD, using tree rings of carbonized logs buried in the tephra in Changbai Mountain, northeast Asia. The reconstructed temperature changes were consistent with previous reconstructions in China and Northern Hemisphere. The influences of large-scale oscillations (e.g., El Niño-Southern Oscillation) on temperature variability were not significantly different between the periods of 745-946 AD preceding the eruption and 1883-2012. However, compared to the paleotemperature of the prior millennium, the temperature changes were more complex with stronger temperature fluctuations, more frequent temperature abruptions, and a weaker periodicity of temperature variance during the last 130 years. These recent changes correspond to long-term anthropogenic influences on regional climate.

Keywords: Carbonized logs; Changbai Mountain; dendroclimatology; Millennium volcanic eruption; temperature reconstruction; tree rings.

1. Introduction

The observed global mean surface temperature for the decade 2011-2020 was ~1.09 ℃ higher than the average over the 1850-1900 period, reflecting the warming trend since the industrial period (IPCC, 2021). Century-wide predictions have been made based on relatively short-term observations, which bear great uncertainties especially at local and regional spatial scales. Different from the short instrumental records, reconstructing long-term climate variability using annually-resolved proxies such as tree rings is important for analyzing the long-term variations in climate and discriminating among natural and anthropogenic factors that drive climate change (Wang et al., 2018). Long-term dendroclimatic reconstructions of temperature are essential to validate global climate models and provide important inputs to understand vegetation succession and vegetation-climate relationships in the region (Schneider et al., 2015).

Tree rings are excellent proxies for high-resolution climate reconstruction (Fritts, 1976). Several millennial-scale annual climate reconstructions have been developed by multiproxy data for the globe(Consortium et al., 2013; Mann et al., 2008; Mann and Jones, 2003), North Hemisphere (Guillet et al., 2017; Moberg et al., 2005; Mann et al., 1999) or North Hemisphere extratropical regions (Schneider et al., 2015; Ljungqvist, 2010). Some millennial temperature reconstructions with very coarse temporal resolution using other proxies were also completed in northeast Asia, e.g., using varved sediment in Lake Sihailongwan (42°17′53″ N, 126°36′59″ E) (Chu et al., 2012). However, the millennial-scale and high-resolution climate reconstructions rarely include tree-ring proxies from northeast Asia due to limited available tree records prior to the last millennium.

The Changbai Mountain is the highest mountain in northeast Asia and encompasses all life zones found along altitudinal gradients from temperate forests to the alpine tundra (Zhou et al., 2005). Tree radial growth is sensitive to climate change in the Changbai Mt which has allowed building several dendroclimatic reconstructions for the past centuries (Du et al., 2018; Lyu et al., 2016; Zhu et al., 2009; Shao and Wu, 1997). The highest peak of Changbai Mt. with origins from an intraplate stratovolcano (Tianchi volcano) located on the border between China and North Korea (Sun et al., 2014). A Plinian eruption occurred around 1000 AD (well-known as the ‘Millennium Eruption’) with a volcanic explosivity index of 7 based on an estimated eruptive column of ~25-35 km and a total tephra volume of ~100 km^3 (Wei et al., 2003; Horn and Schmincke, 2000). The eruption destroyed most plants within a ~50-km-radial area, but many trees buried by volcanic ash became carbonized logs (Cui et al., 1997). These carbonized logs provide a unique material to reconstruct climate of Changbai Mt. prior to the millennium eruption using tree-ring records as climate proxies.

Numerous studies have attempted dating of the Millennium Eruption (Chen et al., 2016; Xu et al., 2013; Yin et al., 2012). Recently, this eruption has been dated to the end of 946 AD using a conspicuous dating marker of the ephemeral burst of cosmogenic radiation in 775 AD (Oppenheimer et al., 2017; Büntgen et al., 2014) and historical documents (Yun, 2013). With this date, carbonized trees provide the opportunity to reconstruct climate before 946 AD in Changbai Mt., a region where the greatest increase in air temperature over China was recorded during the last century (Ding et al., 2007).

Here, we analyze tree rings from the carbonized logs and modern trees on Changbai Mt. to reconstruct and compare temperatures between the three centuries pre-Millennium Eruption and the last two centuries (1883-2012). These temperature reconstructions can reveal the long-term regional climate dynamics in northeastern China or even Northeast Asia and allow characterizing recent features related to anthropogenic climate warming.

2. Material and methods

The Changbai Mt. ranges from 713 to 2691 m a.s.l., and belongs to the temperate continental and mountain climate, with an annual mean temperature ranging from -7.3 to 4.9 ℃ and annual precipitation from 800 to 1800 mm (Du et al., 2018). The period of cambial growth of trees is approximately May to September at low altitudes (e.g., 1000 m a.s.l.) and shortens to June to August at high altitudes (e.g., treeline located at ~2060 m a.s.l.) (Du et al., 2021).

We sampled 55 carbonized trees from two nearby sites on the western slope of Changbai Mt. in 2012 and 2013 (site A, 42°9′ N, 127°52′ E, 1025 m a.s.l., with 33 samples; and site B, 42°5.7′ N, 127°42.4′ E, 892 m a.s.l., with 22 samples) (Figure 1a, b, c). Most of these trees had bark indicating the last year of tree growth was present (Figure 1d). Radiocarbon dating of the wood of the outermost rings of two trees (from sites A and B, respectively; Figure 1a) was conducted in the Accelerator Mass Spectrometry (AMS) Laboratory at Peking University (Table 1) and indicated that these trees died during the Millennium Eruption in 946 AD. Other carbonized trees found and reported in previous studies were also dead in 946 AD (e.g., Oppenheimer et al., 2017; Xu et al., 2013; Yin et al., 2012). Many of these carbonized tree samples were not totally carbonized (Figure 1b) and showed a complete tree trunk (Figure 1c), indicating that little or no transport has occurred from their original location.

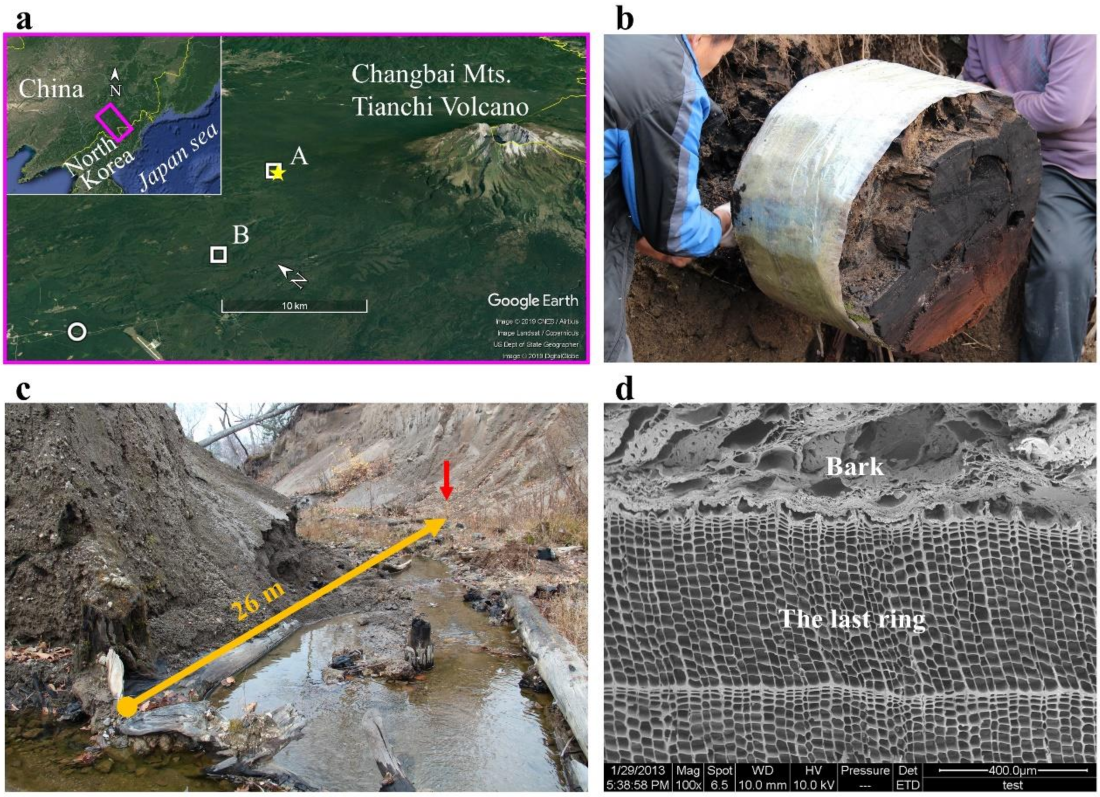

Figure 1. (**a**) Location of the Changbai Mountain and sample sites on Changbai Mt. White squares represent sites where the carbonized logs were found (A, Weidongzhan; B, Xiaoshahe). Yellow star shows the sampling site of the modern forest. White circle indicates the Donggang National Datum Meteorological Station. (**b** and **c**) Context of carbonized logs in the field. Species of logs are *Pinus koraiensis*. (**d**) Cellular characteristics of the outermost tree ring and bark of the carbonized log shown in (b).

Table 1. AMS ^{14}C results of the complete outermost rings of two carbonized logs collected from Weidongzhan (Site A) and Xiaoshahe (Site B) on the western slope of the Changbai Mountain.

Lab ID	Site	AMS ^{14}C age	Tree-ring calibration	Tree-ring calibration

		(yr BP)*	age (AD, 1σ (68.2%))	age (AD, 2σ (95.4%))
BA150220	A	1155±20	780-790 AD (1.0%)	770-970 AD (95.4%)
			820-840 AD (7.4%)	
			860-900 AD (33.8%)	
			910-950 AD (25.9%)	
BA121692	B	1090±20	895-920 AD (24.8%)	890-1020 AD (95.4%)
			945-990 AD (43.4%)	

* AMS ^{14}C ages are dated at the Peking University AMS Laboratory and given in year BP (years before 1950).

We identified the tree species of carbonized trees by analyzing microscopic anatomical features of wood on three planes (cross-sectional, radial, and tangential) (see “**Identifying Korean pine tree species from carbonized trees”** in the Supplement for details). Eighteen of the 55 sample trees were identified as Korean pine (*Pinus koraiensis* Siebold & Zucc.) (Figure S1). However, some small Korean pine was excluded from the chronology development, and only 19 cores from ten Korean pines after the quality control of the cross-dating were finally used for developing chronology. Prior to performing the climate response analyses, we also sampled modern living Korean pines. Core samples from 27 living Korean pine trees located near site A (see Figure 1a) were collected in 2013 and at 1.3 m height using a Pressler increment borer. We used the 19 carbonized Korean pine cores to reconstruct the climate before the Millennium Eruption (946 AD) using the current climate response of Korean pine growth.

Tree-ring width measurements and chronology development of carbonized and living samples were conducted using standard dendrochronological techniques (Cook and Kairiukstis, 2013). The carbonized and living samples were naturally air-dried. The surface of the stem cross section of carbonized trees and the core of living trees was polished with a sandpaper polishing machine, and thick and thin brushes. Then, the tree ring width was identified and recorded by a LINTAB 6 measuring system with an accuracy of 0.001 mm. For each carbonized tree, two cores along one line crossing the pith were measured. Quality of the cross-dating was assessed using the COFECHA program (Holmes, 1983). Core segments having low correlation with the master chronology were excluded from the analysis. Tree ring width series were detrended using polynomial functions (splines with a period of 67% of series length). However, results may be sensitive to the detrending method (Peters et al. 2015). Therefore, to ensure robustness of our results to method choice, age detrending of the ring-width series was also performed by fitting negative exponential curves. Standardized (STD) growth chronologies were developed by calculating robust biweight means using the ARSTAN program version 49 (Cook et al., 2017; Cook, 1985). Then, subsample signal strength (SSS) was used to evaluate the suitability and reliability of chronology data for climate reconstructions (Buras, 2017; Wigley et al., 1984). The SSS > 0.85 was used to determine the robust and maximum chronology length and to ensure the reliability of the reconstructions (Figure S2). This threshold corresponded to a minimum sample depth of 11 samples for the carbonized tree chronology (from 745 AD) and 13 samples for the living tree chronology (from 1883 AD onwards) (Table 2). The dendrochronological characteristics of the STD ring-width chronologies of carbonized and living trees were showed in Table 2.

Table 2. Dendrochronological characteristics of the STD chronologies of carbonized and living trees.

Parameters	Carbonized trees	Modern living trees
Number of cores/trees	19/10	46/24
Time span (SSS > 0.85, year)	745-946	1883-2012
Mean sensitivity	0.163	0.226
Standard deviation	0.288	0.307
First-order autocorrelation coefficient	0.737	0.550
Correlation coefficients of all sequence	0.457	0.210
Mean correlation coefficient in a tree	0.591	0.507
Mean correlation coefficient between trees	0.390	0.194
Signal to Noise Ratio	3.368	3.450
Variance in first eigenvector (%)	59.7	27.9

Instrumental climate data were obtained for the period 1961-2012 from the Donggang

National Datum Meteorological Station (42°6′ N, 127°34.2′ E, 851 m a.s.l., situated 15-22 km apart from the sample sites; source: China Meteorological Data Network, http://data.cma.gov.cn/). We calculated the Pearson correlation coefficients between the STD chronology and different time-scale (monthly, seasonal and annual) climate variables (precipitation, mean temperature, maximum temperature, and minimum temperature) to identify the main climate factors driving tree growth (Figure 2). The radial growth of Korean pine was related to temperature in the pre-growing season onward (Wang et al., 2017; Zhu et al., 2009) and until the end of growing season (September). Moreover, climate may show time-lag effects on tree radial growth (Zhou et al., 2022). Therefore, correlations were calculated from the previous April to current September (Figure 2). Besides, to remove the trend effects, the correlation coefficients between the first-order difference series of chronology and climate variables were also calculated to further explore their relationships (Figure S3).

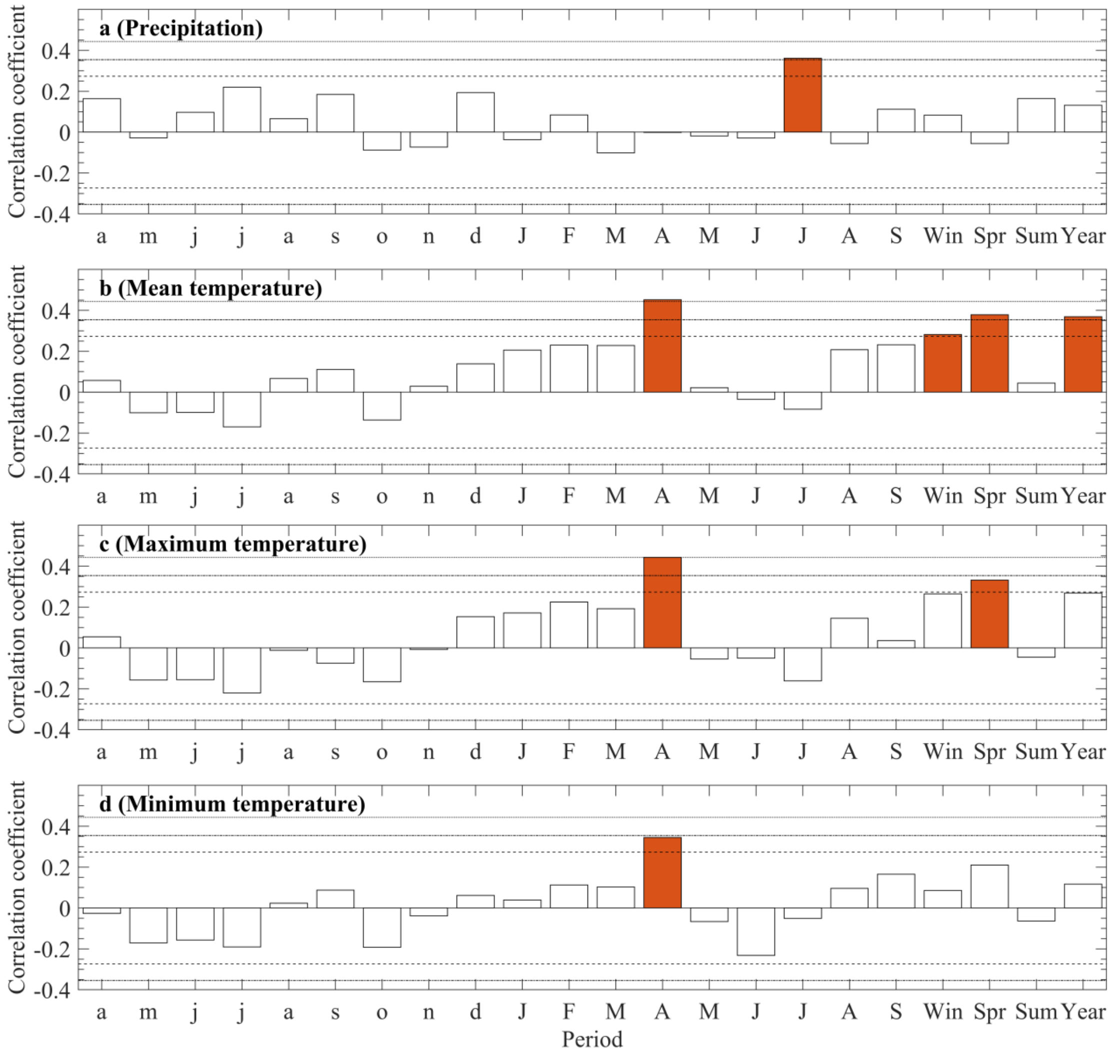

Figure 2. Pearson correlation coefficients between the STD tree-ring chronology and monthly, seasonal and annual (**a**) precipitation, (**b**) mean temperature, (c) maximum temperature, and (d) minimum temperature during 1961-2012. Lowercase and uppercase letter on x axis indicate the months of the previous and current year, respectively. The horizontal dotted, dash-dotted, and dashed lines represent significance levels of 0.001, 0.01, and 0.05, respectively. Bars with significant correlation are filled with red colour.

We used a linear regression model to reconstruct past climate from the STD tree-ring chronology. The reliability of the regression model was evaluated using split sample calibration-validation statistics whereby calibration was conducted for 1961-1986 and validation was done for 1987-2012, after which the periods were switched and the process repeated (Table 3). Model statistics included the Pearson correlation coefficient, coefficient of determination (R^2), reduction of error (RE), coefficient of efficiency (CE), Durbin-Watson text (DW), root-mean-square error (RMSE), and mean absolute error (MAE). Any positive RE/CE is generally accepted as indicative of reasonable skill in the reconstructions (Cook et al., 1994; Briffa et al., 1988; Fritts, 1976). The DW statistic tests the temporal autocorrelation in the residuals between modelled and observed climate data.

Table 3. Calibration/verification statistics of the temperature reconstruction.

	Calibration 1961-1986	Verification 1987-2012	Calibration 1987-2012	Verification 1961-1986	Calibration 1961-2012
Years	26	26	26	26	52
Correlation	0.42	0.45	0.45	0.42	0.45
R^2	0.18	0.20	0.20	0.18	0.20
RE	--	0.25	--	0.24	--
CE	--	0.19	--	0.17	--
DW	2.12	1.88	1.88	2.12	2.01
RMSE	1.51	1.61	1.60	1.51	1.56

MAE	1.27	1.25	1.25	1.28	1.26

Correlation, R^2, and DW were calculated between instrumental April temperature and STD tree-ring width chronology. Reduction of error (RE), coefficient of efficiency (CE), root-mean-square error (RMSE) and mean absolute error (MAE) were calculated between instrumental and reconstructed April temperatures.

To analyze the abrupt changes in temperature between both periods, we calculated the changes in mean state of temperature reconstructions using a heuristic segmentation algorithm (the imposed minimum length of segments is 45 years) developed by Bernaola-Galván et al. (2001). This method has been widely used to determine the abrupt changes in mean state of a chronology (Gong et al., 2006). The significance of the changes was estimated by the *t* test.

Power spectrum analysis was applied to investigate the reasonable periodicities in our climate reconstructions. We used the wavelet analysis with a Morlet wavelet to examine the periodicity of the reconstructed series and to check how periodicity changes through time (Torrence and Compo, 1998). This analysis was separately performed over the two ranges of the reconstructions. We also used the cross wavelet transform analysis (Grinsted et al., 2004) to reveal the correlation and consistency of the periodicity of mean air temperature of Changbai Mt. during 1961-2012 and mean sea surface temperature (SST) of Eastern Tropical Pacific (0 to 10° South and 90°

West to 80 °West) time series (https://psl.noaa.gov/data/timeseries/monthly/NINO12/). These analyses were carried out using the Matlab R2019b software.

3. Results and Discussion

3.1. Temperature reconstruction

Precipitation in all months (except July) and seasons showed no significant correlation with the STD chronology (Figure 2a). This was expected since the study area is wet, and moisture-deficits that limit plant growth are uncommon. In contrast, some monthly, seasonal, and annual mean temperatures significantly affected the growth of Korean pine, especially for the mean temperature in April, which showed a significant ($p < 0.001$) positive correlation ($r = 0.45$) with the STD chronology during 1961-2012 (Figure 2b), indicating that the radial growth of Korean pine is primarily limited by temperature in the month preceding cambial onset. Interestingly, the correlation coefficient between the STD chronology and April mean temperature did not change ($p > 0.01$) during 1961-2012 in the Changbai Mt. (Figure S4). The radial growth of Korean pine was also mostly significantly correlated to the maximum and minimum temperatures in April (Figure 2cd). Similar results were found when the tree-ring width was detrended by fitting the negative exponential curves (Figure S5). Moreover, the correlation coefficients for the first-order difference series indicated that chronologies still have statistically significant and strongest relationship with April temperature (Figure S3). These are similar to the findings for Korean pine growth found in north of Changbai Mt. (Zhu et al., 2009) and more broadly across northeast Asia (Wang et al., 2017). Other species in other cold regions show consistent growth responses to pre-growth temperature as a limiting factor in annual radial growth (e.g., Hinoki cypress (*Chamaecyparis obtuse*) in central Japan (Yonenobu and Eckstein, 2006), Georgei fir (*Abies georgei*) in the southeast Tibetan Plateau (Liang et al., 2009), and Scots pine (*Pinus sylvestris L.*) in northern Poland (Koprowski et al., 2012)). A positive growth response to April temperature can occur due to warming in the period prior to the growing season causing tree dormancy to break early, accelerating the division and enlargement of cambial cells, and extending the length of the growing season (Schweingruber, 1996). The correlation between the STD chronology and spring temperature is also significant, mainly due to the effects of April temperature (Figure 2bc).

The positive RE (0.25) and CE (0.19) statistics for the late verification period and positive RE (0.24) and CE (0.17) statistics for the early verification period indicated reasonable reconstruction skill for both compared sub-periods (Table 3). Therefore, we used the full calibration period for developing April temperature model by calculating the model R^2, DW (Durbin-Watson statistic), RMSE, and MAE (Table 3). The DW statistic calculated over the full calibration period ($DW_{1961\text{-}2012} = 2.01$, $p < 0.01$), achieving a value very close to the optimal value of 2 which indicates no significant autocorrelation in the residuals. The full tree-ring model predicting April temperature was given as:

$$y = 4.34*STD + 1.33 \quad (1);$$

where y is April temperature and *STD* is the standardized tree-ring width index, being the model and the predictor variables significant at $p < 0.01$. The comparison between the reconstructed and instrumental April temperature was showed in Figure 3. The reconstructed April mean temperature showed decreasing trend after 2000, which was different from the results of reconstructed April-July minimum temperature by Lyu et al. (2016) and February-April temperature by Zhu et al. (2009). However, the decreasing trend was coincident with the change in the observed April temperature (Figure 3a). Therefore, the difference of the change in temperature during the last decade between the temperature reconstructions may be due to seasonal diversity or regional difference. Besides, although the reconstruction underestimates the extreme temperatures recorded in some years (e.g., 1965 and 1998), it successfully captures both high and low frequency variations of temperature variability (Figure 3a).

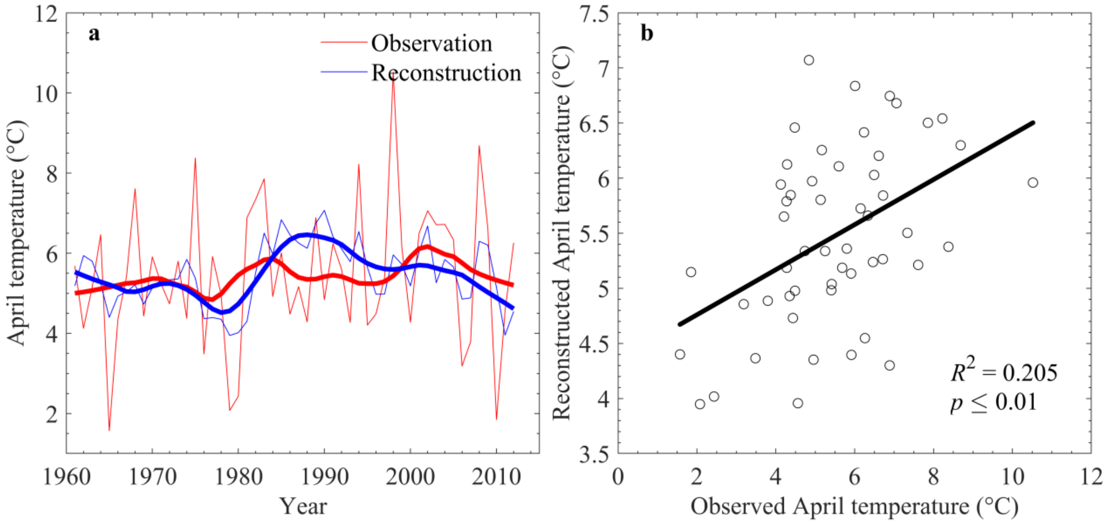

Figure 3. (**a**) Observed (red thin line) and reconstructed (blue thin line) annual April

temperature. Heavy lines are the corresponding 13-year moving averaged temperatures. (**b**) Linear regression between observed and reconstructed temperatures during the period 1961-2012.

3.2. Comparisons between changes in paleoclimate and modern climate

Based on the regression model, we reconstructed the annual April temperature and a 13-year moving average for periods 652-946 AD and 1830-2012 AD (Figure 4a). Truncated periods of reconstructions where SSS is > 0.85 were 745-946 AD and 1883-2012 AD. Our temperature reconstructions did not match well with the previous temperature reconstructions using the varved sediment in Lake Sihailongwan in the Changbai Mt. (Chu et al., 2012), which may be due to age model error inherent in radiocarbon-dated records (Conroy et al., 2010). However, both temperature reconstructions showed coincident decreasing-increasing-decreasing variation during 850-946 AD. For regional scale, our temperature reconstructions generally coincided with the variations of pre-millennial temperature in China (Yang et al., 2002). Interestingly, variations in April temperature reconstructions in both two periods in this study are similar to those observed in summer temperature reconstructions for Northern Hemisphere (Guillet et al., 2017). These temperature reconstructions all display warm periods in 830-850 AD, 1935-1955 AD, 1984-2000s AD, and cold periods in 1830-1840 AD and 1955-1983 AD.

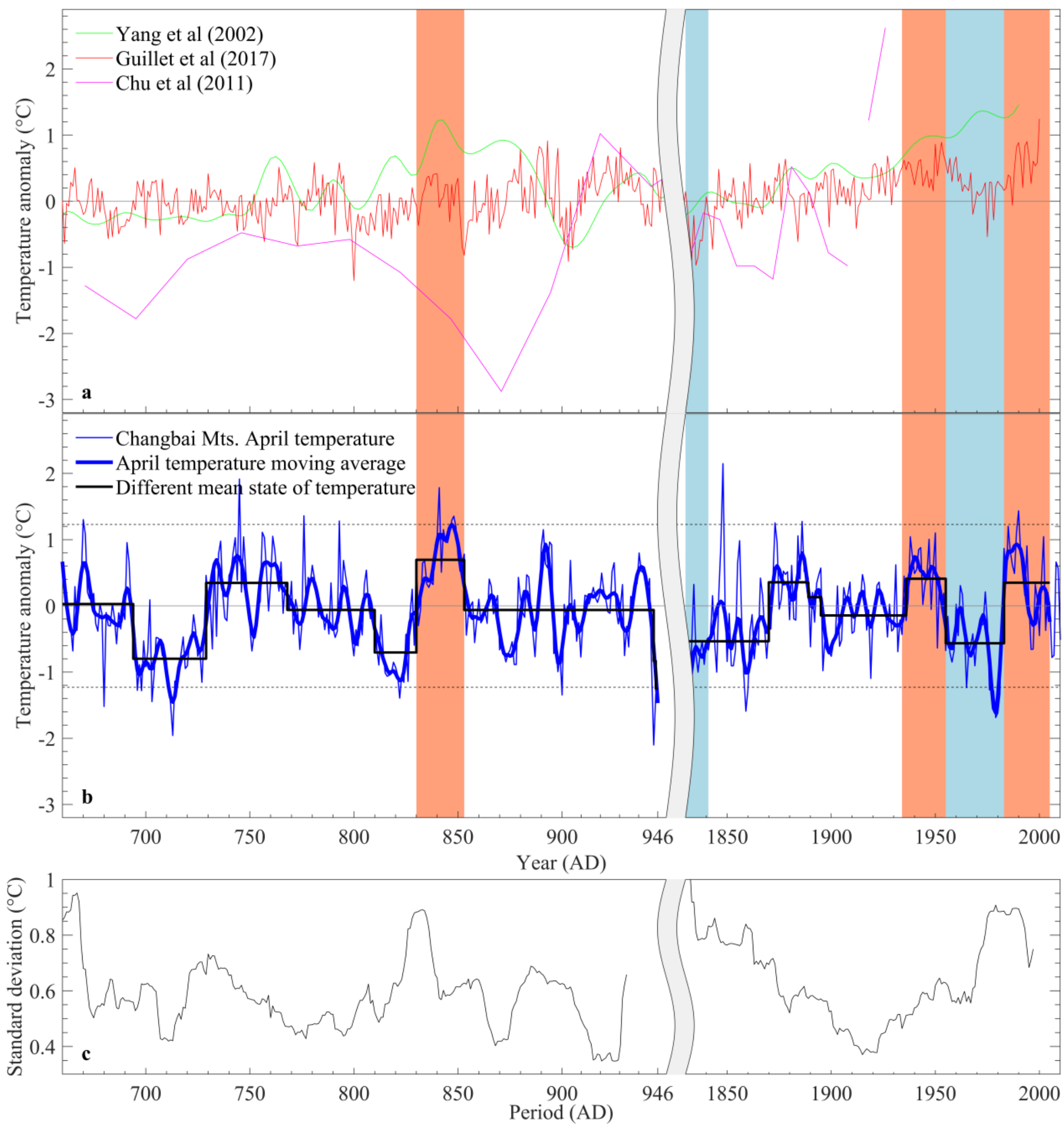

Figure 4. Anomaly of reconstructed temperature in 652-946 AD and 1830-2012 AD for different regions. (**a**) Long-term standardized temperature anomalies in China (“H-res”) (green lines) (Yang et al., 2002), summer temperature anomalies for Northern Hemisphere (red lines) (Guillet et al., 2017), and temperature anomalies using the varved sediment in Lake Sihailongwan in the Changbai Mt. (magenta lines) (Chu et al., 2012). (b) Reconstruction of April temperature anomaly (blue thin lines) with a 13-year moving average (blue bold lines) for Changbai Mt. in this study. The temperature anomaly is relative to the mean during the entire period. Black bold lines

show the changes in mean state of the April temperature reconstructions. (**c**) Time series of standard deviation of 30-year moving window for the April temperature reconstructions in this study. A given period (e.g., 900 AD) represents a standard deviation in 30 years before and after that period (e.g., 886-915 AD).

The standard deviation (s.d.) of reconstructed mean April temperature was 0.61 ℃ during the last 100 years (847-946 AD) before the Millennium Eruption, whereas the standard deviation was 0.69 ℃ for the last 100 years (1913-2012 AD). That is, temperature variance (standard deviation) increased 13% for modern temperature in comparison to the temperature prior to the 946 AD Millennium Eruption. Moreover, the 30-year moving standard deviations showed periodical change and smaller values during the pre-eruption period than those in the last 170 years (Figure 4b). Specifically, the 30-year moving temperature variance showed significant ($p < 0.05$) periodicity of 50-70 years (Figure S6ab). However, there was no significant periodicity of temperature variance during the last 170 years (Figure S6cd).

There were only five periods with significant differences in mean state of temperature during the last ~200 years before the volcano eruption (Figure 4a). The significant warm period in 830-850 AD was widely recognized as warm epoch also by other temperature reconstructions for Northern Hemisphere extratropical areas (e.g., Esper et al., 2002). In contrast, seven periods with significantly different mean temperature states were revealed during the last ~170 years before present. Moreover, five warm years (defined as > 1.5 s.d.; years: 776, 793, 841, 847, 848) and four cold years (defined as < 1.5 s.d.; years: 822, 900, 944, 945) were identified during the last 200 years before the Millennium Eruption, whereas four warm years (1848, 1873, 1886, 1990) and ten cold years (1859, 1860, 1965, 1976, 1977, 1978, 1979, 1980, 1981, 2011) were identified during the last 170 years before present (Figure 4a).

These differences may be partly due to the anthropogenic influences since approximately the beginning of the Industrial Revolution (Gong et al., 2006). For example, the probability of present-day hot extremes increased 1-1.2% relative to pre-Industrial Revolution time in the region of Changbai Mt. Presently, 75% of the moderate hot extremes occurring worldwide are attributable to climate warming, of which the majority are extremely likely to be anthropogenic (Fischer and Knutti, 2015). Higher 30-year standard deviations during the last 170 years than the pre-eruption period may also support the attribution to increased anthropogenic influences on thermal conditions (Figure 4b).

Wavelet analysis indicated significant ($p < 0.05$) periodicity of 3 to 4 years during 770-946 AD (Figure 5ab). Similar periodicities of 3 to 4 years were also found in previous analyses of instrumental and reconstructed temperatures (Zhang et al., 2013; Yu et al., 2013; Chen et al., 2010). Although our temperature reconstructions did not contain the significant ($p < 0.05$) quasi-11-year periodicity (e.g., Li et al., 2011) during the entire period, the significant ($p < 0.05$) quasi-11-year periodicity in 880-910 AD and the non-significant quasi-11-year period in 840-870 AD were found. Significantly short periodicities are typically associated with El Niño-Southern Oscillation (ENSO) (Stone et al., 1998; Allan et al., 1996) and temperature in March to May in northeast China is affected by ENSO (Yuan and Yang, 2012). Moreover, the changes in temperature in northeast China correspond to the quasi-4-year changes in sea surface temperature in the central and eastern Pacific Ocean, suggesting a close link between temperature variation in northeast China and the ENSO cycle (Zhu et al., 2004). For example, the significant ($p < 0.05$) quasi-4-year periodicity was found during the last ~120 years in the Changbai Mt. (Figure 5cd). Moreover, the cross wavelet transform analysis showed that there was significant high common power in a quasi-4-year band for three periods during 1961-2012 for temperature in Changbai Mt. and sea surface temperature in Eastern Tropical Pacific (Figure S7). These results indicate that the effects of some large-scale oscillations (e.g., ENSO) on paleo- and modern- temperature continue to be important to the climate forcing in the region of Changbai Mt.

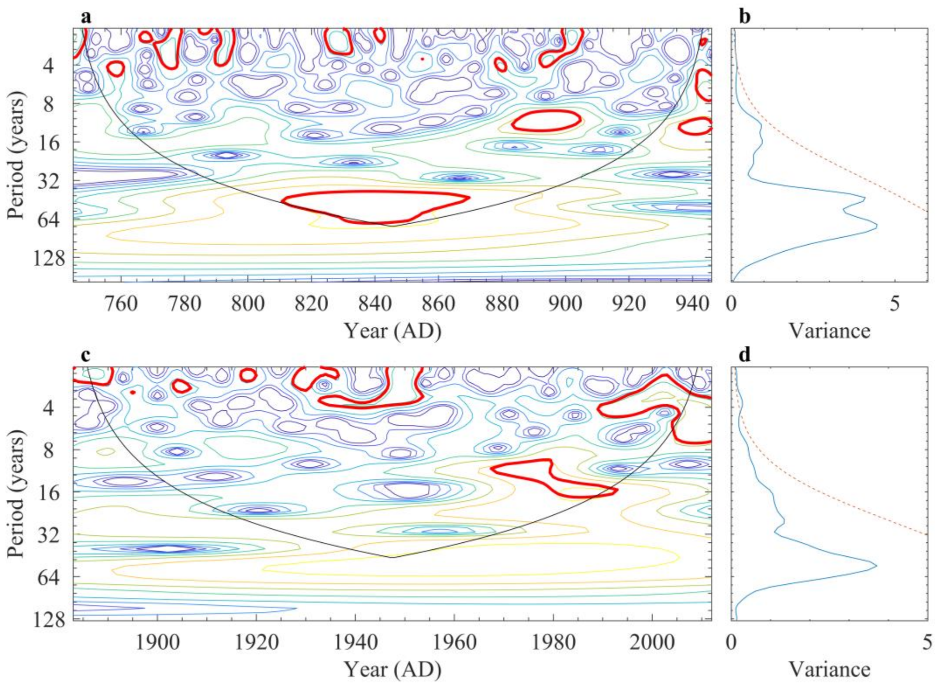

Figure 5. (**a**, **c**) Wavelet power spectrum of the reconstructed April temperature from (a) carbonized and (c) modern trees. The power has been scaled by the global wavelet spectrum. Bold red contour is the 95% confidence level using a red-noise (autoregressive lag1) background spectrum. (**b**, **d**) The global wavelet power spectrum (light blue line) for (b) carbonized trees-based and (d) modern trees-based temperature reconstruction. Dashed lines represent a significance of 0.05.

4. Conclusions

We presented a new 202-year reconstruction of April temperature before the Millennium Eruption occurred in 946 AD at Changbai Mt. using unique tree-ring proxies of carbonized logs buried in the tephra, which was compared to that of living trees growing during the last 130 years. Temperature reconstructions correspond well with previous large-regional temperature reconstructions. Our results showed that, although the influences of some internal variability (e.g., ENSO) on variation in temperature do not change between the periods, the changes in modern temperatures become more complex (e.g., increased variation and abrupt changes, and weakening in periodicity of temperature variance) than those in period prior to 946 AD likely due to anthropogenic influences. The present study provides tree-ring proxies for climate reconstructions in northeast Asia for the last millennium. Documentation of these features is important for understanding long-term regional climate dynamics and analyzing the millennial-scale changes in vegetation-climate relationship in northeast Asia.

Data availability

Tree-ring chronology and climate data used in this study are archived at ZENODO: https://doi.org/10.5281/zenodo.6633856. They can also be provided by the corresponding author.

Authors' contributions

H.D., Z.W., and H.S.H. conceived and led this study. Tree rings and observation data collection was led by H.D. and S.Z. Analyses and the first draft was carried out by H.D. and M.S., and all authors contributed to revising subsequent manuscripts.

Declaration of Competing Interest

The authors declare that they have no conflict of interest.

Acknowledgments

We acknowledge support from the National Natural Science Foundation of China (grant number 42271100; U19A2023) and the Fundamental Research Funds for the Central Universities (grant number 2412020FZ002).

References

Allan, R., Lindesay, J., and Parker, D.: El Niño southern oscillation & climatic variability, CSIRO Publishing, Collingwood, 405 pp, 1996.

Bernaola-Galván, P., Ivanov, P. C., Nunes Amaral, L. A., and Stanley, H. E.: Scale Invariance in the Nonstationarity of Human Heart Rate, Phys. Rev. Lett., 87, 168105, https://doi.org/10.1103/PhysRevLett.87.168105, 2001.

Briffa, K. R., Jones, P. D., Pilcher, J. R., and Hughes, M. K.: Reconstructing Summer Temperatures in Northern Fennoscandinavia Back to A.D. 1700 Using Tree-Ring Data From Scots Pine, Arct. Alp. Res., 20, 385-394, https://doi.org/10.1080/00040851.1988.12002691, 1988.

Büntgen, U., Wacker, L., Nicolussi, K., Sigl, M., Güttler, D., Tegel, W., Krusic, P. J., and Esper, J.: Extraterrestrial confirmation of tree-ring dating, Nat. Clim. Change, 4, 404, https://doi.org/10.1038/nclimate2240, 2014.

Buras, A.: A comment on the expressed population signal, Dendrochronologia, 44, 130-132, https://doi.org/10.1016/j.dendro.2017.03.005, 2017.

Chen, S., Shi, Y., Guo, Y., and Zheng, Y.: Temporal and spatial variation of annual mean air temperature in arid and semiarid region in northwest China over a recent 46 year period, J. Arid Land, 2, 87-97, https://doi.org/10.3724/SP.J.1227.2010.00087, 2010.

Chen, X.-Y., Blockley, S. P. E., Tarasov, P. E., Xu, Y.-G., McLean, D., Tomlinson, E. L., Albert, P. G., Liu, J.-Q., Müller, S., Wagner, M., and Menzies, M. A.:

Clarifying the distal to proximal tephrochronology of the Millennium (B–Tm) eruption, Changbaishan Volcano, northeast China, Quat. Geochronol., 33, 61-75, https://doi.org/10.1016/j.quageo.2016.02.003, 2016.

Chu, G., Sun, Q., Wang, X., Liu, M., Lin, Y., Xie, M., Shang, W., and Liu, J.: Seasonal temperature variability during the past 1600 years recorded in historical documents and varved lake sediment profiles from northeastern China, The Holocene, 22, 785-792, https://doi.org/10.1177/0959683611430413, 2012.

Conroy, J. L., Overpeck, J. T., and Cole, J. E.: El Niño/Southern Oscillation and changes in the zonal gradient of tropical Pacific sea surface temperature over the last 1.2 ka, PAGES News, 18, 32-34, 2010.

Cook, E. R.: A time series analysis approach to tree-ring standardization, Graduate College, University of Arizona, Tucson, 1985.

Cook, E. R. and Kairiukstis, L. A.: Methods of Dendrochronology: Applications in the Environmental Sciences, Springer Netherlands, 394 pp, https://doi.org/10.1007/978-94-015-7879-0, 2013.

Cook, E. R., Briffa, K. R., and Jones, P. D.: Spatial regression methods in dendroclimatology: A review and comparison of two techniques, Int. J. Climatol., 14, 379-402, https://doi.org/10.1002/joc.3370140404, 1994.

Cook, E. R., Krusic, P. J., Peters, K., and Holmes, R. L.: Program ARSTAN (version 49), Autoregressive tree–ring standardization program. Tree–Ring Laboratory of Lamont–Doherty Earth Observatory, USA, 2017.

Cui, Z., Zhang, S., and Tian, J.: The study on volcanic eruption and forest conflagration since holocene quaternary in Changbai Mt., Geogr. Res., 16, 92-97, 1997.

Ding, Y., Ren, G., Zhao, Z., Xu, Y., Luo, Y., Li, Q., and Zhang, J.: Detection, causes and projection of climate change over China: An overview of recent progress, Adv. Atmos. Sci., 24, 954-971, https://doi.org/10.1007/s00376-007-0954-4, 2007.

Du, H., Li, M.-H., Rixen, C., Zong, S., Stambaugh, M., Huang, L., He, H. S., and Wu, Z.: Sensitivity of recruitment and growth of alpine treeline birch to elevated temperature, Agric. For. Meteorol., 304-305, 108403, https://doi.org/10.1016/j.agrformet.2021.108403, 2021.

Du, H., Liu, J., Li, M.-H., Büntgen, U., Yang, Y., Wang, L., Wu, Z., and He, H. S.: Warming-induced upward migration of the alpine treeline in the Changbai Mountains, northeast China, Global Change Biol., 24, 1256-1266, https://doi.org/10.1111/gcb.13963, 2018.

Esper, J., Cook, E. R., and Schweingruber, F. H.: Low-Frequency Signals in Long Tree-Ring Chronologies for Reconstructing Past Temperature Variability, Science, 295, 2250-2253, https://doi.org/10.1126/science.1066208, 2002.

Fischer, E. M. and Knutti, R.: Anthropogenic contribution to global occurrence of heavy-precipitation and high-temperature extremes, Nat. Clim. Change, 5, 560, https://doi.org/10.1038/nclimate2617, 2015.

Fritts, H. C.: Tree rings and climate, Elsevier, New York, 1976.

Gong, Z.-Q., Feng, G.-L., Wan, S.-Q., and Li, J.-P.: Analysis of features of climate change of Huabei area and the global climate change based on heuristic segmentation algorithm, Acta Phys. Sinica, 55, 477, https://doi.org/10.7498/aps.55.477, 2006.

Grinsted, A., Moore, J. C., and Jevrejeva, S.: Application of the cross wavelet transform and wavelet coherence to geophysical time series, Nonlin. Processes Geophys., 11, 561-566, https://doi.org/10.5194/npg-11-561-2004, 2004.

Guillet, S., Corona, C., Stoffel, M., Khodri, M., Lavigne, F., Ortega, P., Eckert, N., Sielenou, P. D., Daux, V., Churakova , Olga V., Davi, N., Edouard, J.-L., Zhang, Y., Luckman, Brian H., Myglan, V. S., Guiot, J., Beniston, M., Masson-Delmotte, V., and Oppenheimer, C.: Climate response to the Samalas volcanic eruption in 1257 revealed by proxy records, Nat. Geosci., 10, 123, https://doi.org/10.1038/ngeo2875, 2017.

Holmes, R. L.: Computer-assisted quality control in tree-ring dating and measurement, Tree-Ring Bull., 43, 69-78, 1983.

Horn, S. and Schmincke, H.-U.: Volatile emission during the eruption of Baitoushan Volcano (China/North Korea) ca. 969 AD, Bull. Volcanol., 61, 537-555, https://doi.org/10.1007/s004450050004, 2000.

IPCC: Summary for Policymakers. In: Climate Change 2021: The Physical Science

Basis. Contribution of Working Group I to the Sixth Assessment Report of the Intergovernmental Panel on Climate Change [Masson-Delmotte, V., P. Zhai, A. Pirani, S. L. Connors, C. Péan, S. Berger, N. Caud, Y. Chen, L. Goldfarb, M. I. Gomis, M. Huang, K. Leitzell, E. Lonnoy, J.B.R. Matthews, T. K. Maycock, T. Waterfield, O. Yelekçi, R. Yu and B. Zhou (eds.)]. Cambridge University Press. In Press, 2021.

Koprowski, M., Przybylak, R., Zielski, A., and Pospieszyńska, A.: Tree rings of Scots pine (Pinus sylvestris L.) as a source of information about past climate in northern Poland, Int. J. Biometeorol., 56, 1-10, https://doi.org/10.1007/s00484-010-0390-5, 2012.

Li, Z., Shi, C. M., Liu, Y., Zhang, J., Zhang, Q., and Ma, K.: Summer mean temperature variation from 1710–2005 inferred from tree-ring data of the Baimang Snow Mountains, northwestern Yunnan, China, Clim. Res., 47, 207-218, https://doi.org/10.3354/cr01012, 2011.

Liang, E. Y., Shao, X. M., and Xu, Y.: Tree-ring evidence of recent abnormal warming on the southeast Tibetan Plateau, Theor. Appl. Climatol., 98, 9-18, https://doi.org/10.1007/s00704-008-0085-6, 2009.

Ljungqvist, F. C.: A new reconstruction of temperature variability in the extra-tropical northern hemisphere during the last two millennia, Geogr. Ann. Ser. A Phys. Geogr., 92, 339-351, https://doi.org/10.1111/j.1468-0459.2010.00399.x, 2010.

Lyu, S., Li, Z., Zhang, Y., and Wang, X.: A 414-year tree-ring-based April–July minimum temperature reconstruction and its implications for the extreme climate events, northeast China, Clim. Past, 12, 1879-1888, https://doi.org/10.5194/cp-12-1879-2016, 2016.

Mann, M. E. and Jones, P. D.: Global surface temperatures over the past two millennia, Geophys. Res. Lett., 30, https://doi.org/10.1029/2003GL017814, 2003.

Mann, M. E., Bradley, R. S., and Hughes, M. K.: Northern hemisphere temperatures during the past millennium: inferences, uncertainties, and limitations, Geophys. Res. Lett., 26, 759-762, 1999.

Mann, M. E., Zhang, Z., Hughes, M. K., Bradley, R. S., Miller, S. K., Rutherford, S., and Ni, F.: Proxy-based reconstructions of hemispheric and global surface temperature variations over the past two millennia, P. Natl. Acad. Sci. USA, 105, 13252, https://doi.org/10.1073/pnas.0805721105, 2008.

Moberg, A., Sonechkin, D. M., Holmgren, K., Datsenko, N. M., and Karlén, W.: Highly variable Northern Hemisphere temperatures reconstructed from low- and high-resolution proxy data, Nature, 433, 613-617, https://doi.org/10.1038/nature03265, 2005.

Oppenheimer, C., Wacker, L., Xu, J., Galván, J. D., Stoffel, M., Guillet, S., Corona, C., Sigl, M., Di Cosmo, N., Hajdas, I., Pan, B., Breuker, R., Schneider, L., Esper, J., Fei, J., Hammond, J. O. S., and Büntgen, U.: Multi-proxy dating the ‘Millennium Eruption’ of Changbaishan to late 946 CE, Quat. Sci. Rev., 158, 164-171, https://doi.org/10.1016/j.quascirev.2016.12.024, 2017.

PAGES 2k Consortium: Continental-scale temperature variability during the past two millennia, Nat. Geosci., 6, 339, https://doi.org/10.1038/ngeo1797, 2013.

Peters, R. L., Groenendijk, P., Vlam, M., and Zuidema, P. A.: Detecting long-term growth trends using tree rings: a critical evaluation of methods. Global Change Biol., 21, 2040-2054, https://doi.org/10.1111/gcb.12826, 2015.

Schneider, L., Smerdon, J. E., Büntgen, U., Wilson, R. J. S., Myglan, V. S., Kirdyanov, A. V., and Esper, J.: Revising midlatitude summer temperatures back to A.D. 600 based on a wood density network, Geophys. Res. Lett., 42, 4556-4562, https://doi.org/10.1002/2015GL063956, 2015.

Schweingruber, F. H.: Tree rings and environment: dendroecology, Paul Haupt AG Bern, Berne, 609 pp, 1996.

Shao, X. M. and Wu, X. D.: Reconstruction of climate change on Changbai Mountain, northeast China using tree-ring data, Quaternary Science, 1, 76-85 (in Chinese with English abstract), 1997.

Stone, L., Saparin, P. I., Huppert, A., and Price, C.: El Niño Chaos: The role of noise and stochastic resonance on the ENSO cycle, Geophys. Res. Lett., 25, 175-178, https://doi.org/10.1029/97GL53639, 1998.

Sun, C., You, H., Liu, J., Li, X., Gao, J., and Chen, S.: Distribution, geochemistry and age of the Millennium eruptives of Changbaishan volcano, Northeast China — A review, Frontiers of Earth Sci., 8, 216-230, https://doi.org/10.1007/s11707-014-0419-x, 2014.

Torrence, C. and Compo, G. P.: A Practical Guide to Wavelet Analysis, Bull. Am. Meteorol. Soc., 79, 61-78, https://doi.org/10.1175/1520-0477(1998)079<0061:APGTWA>2.0.CO;2, 1998.

Wang, J., Yang, B., Osborn, T. J., Ljungqvist, F. C., Zhang, H., and Luterbacher, J.: Causes of East Asian Temperature Multidecadal Variability Since 850 CE, Geophys. Res. Lett., 45, 13,485-13,494, https://doi.org/10.1029/2018GL080725, 2018.

Wang, X., Zhang, M., Ji, Y., Li, Z., Li, M., and Zhang, Y.: Temperature signals in tree-ring width and divergent growth of Korean pine response to recent climate warming in northeast Asia, Trees, 31, 415-427, https://doi.org/10.1007/s00468-015-1341-x, 2017.

Wei, H., Sparks, R. S. J., Liu, R., Fan, Q., Wang, Y., Hong, H., Zhang, H., Chen, H., Jiang, C., Dong, J., Zheng, Y., and Pan, Y.: Three active volcanoes in China and their hazards, J. Asian Earth Sci., 21, 515-526, https://doi.org/10.1016/S1367-9120(02)00081-0, 2003.

Wigley, T. M. L., Briffa, K. R., and Jones, P. D.: On the Average Value of Correlated Time Series, with Applications in Dendroclimatology and Hydrometeorology, J. Clim. Appl. Meteorol., 23, 201-213, https://doi.org/10.1175/1520-0450(1984)023<0201:OTAVOC>2.0.CO;2, 1984.

Xu, J., Pan, B., Liu, T., Hajdas, I., Zhao, B., Yu, H., Liu, R., and Zhao, P.: Climatic impact of the Millennium eruption of Changbaishan volcano in China: New insights from high-precision radiocarbon wiggle-match dating, Geophys. Res. Lett., 40, 54-59, https://doi.org/10.1029/2012GL054246, 2013.

Yang, B., Braeuning, A., Johnson, K. R., and Shi, Y.: General characteristics of temperature variation in China during the last two millennia, Geophys. Res. Lett., 29, L014485, https://doi.org/10.1029/2001GL014485, 2002.

Yin, J., Jull, A. J. T., Burr, G. S., and Zheng, Y.: A wiggle-match age for the Millennium eruption of Tianchi Volcano at Changbaishan, Northeastern China, Quat. Sci. Rev., 47, 150-159, https://doi.org/10.1016/j.quascirev.2012.05.015, 2012.

Yonenobu, H. and Eckstein, D.: Reconstruction of early spring temperature for central Japan from the tree-ring widths of Hinoki cypress and its verification by other proxy records, Geophys. Res. Lett., 33, L10701, https://doi.org/10.1029/2006GL026170, 2006.

Yu, S., Yuan, Y., Wei, W., Chen, F., Zhang, T., Shang, H., Zhang, R., and Qing, L.: A 352-year record of summer temperature reconstruction in the western Tianshan Mountains, China, as deduced from tree-ring density, Quat. Res., 80, 158-166, https://doi.org/10.1016/j.yqres.2013.05.005, 2013.

Yuan, Y. and Yang, S.: Impacts of Different Types of El Niño on the East Asian

Climate: Focus on ENSO Cycles, J. Clim., 25, 7702-7722, https://doi.org/10.1175/JCLI-D-11-00576.1, 2012.

Yun, S.-H.: Volcanological Interpretation of Historical Eruptions of Mt. Baekdusan Volcano, J. Korean Earth Sci. Soc., 34, 456-469, 2013.

Zhang, T., Yuan, Y., Liu, Y., Wei, W., Zhang, R., Chen, F., Yu, S., Shang, H., and Qin, L.: A tree-ring based temperature reconstruction for the Kaiduhe River watershed, northwestern China, since A.D. 1680: Linkages to the North Atlantic Oscillation, Quat. Int., 311, 71-80, https://doi.org/10.1016/j.quaint.2013.07.026, 2013.

Zhou, Y., Liu, L., Zhang, M., and Yu, J.: Medicinal plant resources and their diversity in Changbai Mountain National Nature Reserve, Scientia Silvae Sinicae, 41, 57-64, 2005.

Zhou, Y., Yi, Y., Liu, H., Song, J., Jia, W., and Zhang, S.: Altitudinal trends in climate change result in radial growth variation of Pinus yunnanensis at an arid-hot valley of southwest China, Dendrochronologia, 71, 125914, https://doi.org/https://doi.org/10.1016/j.dendro.2021.125914, 2022.

Zhu, H. F., Fang, X. Q., Shao, X. M., and Yin, Z. Y.: Tree ring-based February–April temperature reconstruction for Changbai Mountain in Northeast China and its implication for East Asian winter monsoon, Clim. Past, 5, 661-666, https://doi.org/10.5194/cp-5-661-2009, 2009.

Zhu, Y., Chen, L., and Yu, R.: Analysis of the relationship between the China anomalous climate variation and ENSO cycle on the quasi-four-year scale, J. Trop. Meteorol., 19, 345-356, https://doi.org/10.3969/j.issn.1006-8775.2004.01.001, 2004.